Multiphoton FLIM in cosmetic clinical research

Ana-Maria Pena, Etienne Decencière, Sébastien Brizion, Steeve Victorin, Serge Koudoro, Thérèse Baldeweck, Emmanuelle Tancrède-Bohin

Ana-Maria Pena, Etienne Decencière, Sébastien Brizion,
Steeve Victorin, Serge Koudoro, Thérèse Baldeweck,
and Emmanuelle Tancrède-Bohin

19 Multiphoton FLIM in cosmetic clinical research

Abstract: There is an increasing need in cosmetic clinical research for non-invasive, high content, skin imaging techniques offering the possibility on the one hand, to avoid performing invasive biopsies, and on the other hand, to supply a maximum of information on the skin state throughout a study, especially before, during and after product application. Multiphoton microscopy is one of these techniques compatible with *in vivo* human skin investigations, allowing human skin three-dimensional (3D) structure to be characterized with sub-µm resolution. In association with fluorescence lifetime imaging (FLIM) and specific 3D-image processing, one can extract several quantitative parameters characterizing skin constituents in terms of morphology, density and organization. Various intracellular and extracellular constituents present specific endogenous signals enabling a non-invasive visualization of the 3D structure of epidermal and superficial dermal layers. Multiphoton FLIM applications in the cosmetic field range from knowledge to evaluation studies. Knowledge studies aim to acquire a better knowledge of skin differences appearing with aging, solar exposure or between the different skin phototypes. Evaluation studies deal with the efficacy of cosmetic anti-aging or whitening ingredients. The goal of this chapter is not to give a literature review of multiphoton FLIM applications in cosmetic clinical research, but rather to acquaint the reader with the quantitative 3D information afforded by multiphoton FLIM imaging of human skin and its interest in cosmetic clinical research.

19.1 Multiphoton fluorescence lifetime imaging of *in vivo* human skin

In dermatology, skin imaging has always found a privileged position in the scientific literature, for teaching purposes or for the monitoring of the patient, owing to the direct access to the skin. Techniques such as ultrasound, magnetic resonance imaging, optical coherence tomography or *in vivo* confocal microscopy have offered new opportunities for skin imaging not only at its surface but also in depth. Today, the development of non-invasive skin imaging methods, which can be applied *in vivo* on human volunteers, allowing the replacement of biopsies in a number of situations, avoiding their renewal for treatment monitoring, permitting to guide a surgical procedure or to acquire new knowledge on skin constituents, is still a major objective for dermatologists.

https://doi.org/10.1515/9783110429985-021

Similar needs exist in cosmetic clinical research: we are looking for non-invasive, high content, large field of view, high resolution 3D skin imaging techniques offering the possibility, on the one hand, to avoid performing invasive biopsies and, on the other hand, to supply a maximum of information on the skin state throughout a study: before, during and after product application. The most recent imaging techniques offer the subcellular resolution required for the detailed observation of skin. Some of them may also provide access to a three-dimensional *in vivo* functional imaging in real time [1]. Among these, multiphoton microscopy has gradually emerged as the most suitable technique to image skin constituents at the subcellular level *in vivo* on human volunteers. Indeed, multiphoton microscopy is compatible with *in vivo* human skin investigations, allowing human skin 3D structure to be characterized with sub-µm resolution. It offers the possibility to image the cellular and extracellular matrix components non-invasively, by taking advantage of intrinsic multiphoton signals: second-harmonic generation (SHG) created by fibrillar collagens and two-photon excited fluorescence (2PEF) emitted by keratin, nicotinamide adenine dinucleotide (NADH), flavin adenine dinucleotide (FAD), melanin, or elastin [2–7].

Multiphoton microscopy is a form of laser scanning microscopy that uses localized two-photon excitation to produce signals only at the focal point of the objective [8, 9]. The principle of two-photon absorption phenomenon was theoretically demonstrated by Maria Göppert-Mayer in 1931 [10, 11], experimentally proved 30 years later by Kaiser and Garrett [12] with the advent of laser sources. In the 1970s, C. Sheppard and R. Kompfner proposed the construction of a nonlinear laser microscope, built in the 1990s by Denk *et al.* [13]. The concept is based on the idea that two energy-equal near-infrared (NIR) photons can simultaneously be absorbed by a molecule, and produce an excitation equivalent to the absorption of a single photon in the ultraviolet/visible range. Each NIR photon provides half the energy needed to excite the molecule from the fundamental state to the excited state (see Fig. 19.1). The excitation results in the subsequent emission of a fluorescence photon, typically at a higher energy, smaller wavelength, as compared to the infrared (IR) photons. As two photons are required for excitation, the two-photon excited fluorescence signal intensity is proportional to the square of the excitation intensity. This nonlinear dependence on excitation intensity affords a 3D localization of the excitation and emission, confined at the focal point of the objective lens in a sub-femtoliter volume. Indeed, as the probability of two-photon absorption is extremely low, such phenomenon is only possible if the sample is excited with a high power density (MW/cm^2 to GW/cm^2). This can be achieved by focusing the photons both temporally (using IR femtoseconds–fs pulsed lasers that deliver ultra-short laser pulses with a duration of $\approx$ 100 fs) and spatially (at the focal point of the objective lens). This intrinsic "optical sectioning" is the key advantage of multiphoton microscopy over confocal microscopy, which employs additional elements such as pinholes to reject out-of-focus fluorescence. The excitation volume is then scanned in two or three dimensions in the sample to acquire 2D or 3D images.

Multiphoton microscopy presents several other advantages: superior imaging depth within biological tissues as IR light penetrates deeper in the skin than UV/VIS light, less photobleaching and phototoxicity as confined to the excitation volume. Furthermore, it provides additional contrast modes with increased specificity, such as the second harmonic generation, a coherent second-order nonlinear process, forbidden in centrosymmetric media and implying no absorption phenomenon. In the skin, the SHG signal is obtained from dense and ordered macromolecular structures such as fibrillar collagens [14]. SHG microscopy is sensitive to the organization of collagen molecules rather than to the collagen type [14] and probes collagen macromolecular structure at the micrometer scale, which makes it a powerful technique to study collagen organization in biological tissues. Both 2PEF and SHG signals can be excited using the same laser source and detected separately based on their spectral difference. Simultaneous recording of 2PEF and SHG signals enable multimodal imaging of epidermis and superficial dermis up to a depth of about 160–200 μm depending on the body region.

Fluorescence lifetime imaging microscopy [15] brings another dimension to multiphoton microscopy: in association with 2PEF imaging it offers an "additional" mode of contrast with increased specificity offering an insight into the type of fluorophores contributing to the detected signal. Fluorophores with similar emission spectra can be differentiated by FLIM provided that they present different fluorescence lifetimes. Fluorescence lifetime (τ) is a measure of the average time that the fluorophore remains in the excited state following excitation. The excited state decays back to the ground state in a statistical manner. This fluorescence decay has an exponential shape for simple molecules. In skin, the autofluorescence signal within the sub-femtoliter excitation volume comes from a variety of fluorophores and the fluorescence decay typically shows a bi-exponential behavior:

$$Photon\ count(t) = a_1 e^{-t/\tau_1} + a_2 e^{-t/\tau_2},$$

where τ_1 and τ_2 are respectively the fast and slow lifetimes and a_1 and a_2 their amplitudes.

The skin endogenous fluorophores present lifetimes on the order of hundreds of picoseconds (e.g. melanin, free NADH, bound FAD) to nanoseconds (see [16] and included references). The fluorescence lifetime is independent of fluorophore concentration, but depends on the local microenvironment of the molecule that is, for example, pH, binding status, conformational changes.

As an example, the lifetimes of NADH and FAD, two coenzymes involved in cell metabolic activity, differ substantially depending on whether they are free or bound to proteins. The two-photon excited fluorescence intensities of NADH and FAD and especially the "RedOx ratio" (defined as the ratio of the 2PEF intensities of NADH and FAD, or NADH/(NADH + FAD)) can be used as an indicator of the oxidation-reduction potential of a cell, a non-invasive optical metabolic index allowing to assess the changes in metabolic activity. This type of functional information was initially evidenced in

the 1960s by Chance *et al.* in isolated cells [17]. Fluorescence lifetime imaging offers additional functional information in terms of preferred energy production pathways (glycolysis, Krebs cycle, oxidative phosphorylation) by the measuring of the ratio of free and protein-bound NADH and free and protein-bound FAD. A detailed review of the role of NADH and FAD in the metabolic process as well as of the advantages and limitations of two-photon excited fluorescence lifetime imaging to assess the metabolic state is given by Georgakoudi and Quinn in reference [18] and included citations.

Usually NADH and FAD redox ratio imaging and FLIM imaging both require long acquisition times: firstly, due to the fact that an optimal excitation of these two chromophores implies a sequential imaging at ≈ 740 nm for NADH and ≈ 900 nm for FAD, secondly, because NADH and FAD imaging implies different image acquisition times due to their different mitochondrial concentration (orders of magnitude higher for NADH as compared to FAD) and lastly, because FLIM analysis requires an increased number of photons per pixel (hundreds of photons/pixel for a bi-exponential decay). For all these reasons, clinical trials dealing with multiphoton FLIM assessment of the metabolic activity in human volunteers involve mostly a single excitation wavelength, around 760 nm, convenient for NADH imaging.

Fluorescence lifetime imaging affords also a specific detection of melanin, the pigment that gives the color of the skin. Melanin detection can of course be performed by 2PEF imaging in the basal layers of epidermis (highly concentrated melanin regions show 2PEF intensities stronger than that of other endogenous fluorophores). This works satisfactorily in the basal and supra-basal layers as demonstrated with the study of corticosteroids effects [19]. But this type of intensity-based detection is not always satisfactory. First, the signal intensity may be disrupted by other fluorophores also creating intense 2PEF signals (e.g., keratin in the *stratum corneum*), and second, it does not take into account pixels with low melanin concentration of a fluorescence intensity comparable to that of other endogenous fluorophores. A more specific detection can be done by FLIM, as melanin presents an extremely fast decay component (< 0.1 ns). However, melanin detection in the whole epidermis with FLIM is too long to be performed on human volunteers, and in practice is limited to selected 2D slices, obtained at a depth chosen by the operator.

Another approach, combining multiphoton and FLIM, called Pseudo-FLIM, can be used to specifically detect melanin from multiphoton FLIM-like data compatible with 3D *in vivo* acquisitions on human volunteers [20, 21]. The main idea is to bin the fluorescence photons in a reduced number of time channels either at the acquisition or afterwards during processing and to calculate the slope of the decay. By applying a threshold to keep the high slope values (i.e. short lifetimes), one can identify melanin pixels as melanin presents a very short ($\tau_1 < 0.1$ ns) and predominant ($a_1 > 90\,\%$) lifetime component. As this analysis requires only a few photons per pixel (≈ 30), it results in a short image acquisition time (16 µs/pixel) compatible with 3D imaging on humans.

In the literature, many contributions focus on multiphoton/FLIM imaging of normal human skin, characterized either *ex vivo* or *in vivo*. The reader can have an insight on the *in vivo* work that started more than 20 years ago and at the evolution of the imaging instruments by consulting the references [2, 6, 8, 16, 22–44]. The first multiphoton/FLIM data of human skin *in vivo* were obtained in the 1990s by and Masters *et al.* with a homemade microscope on the forearm of one of the authors [2]. Nowadays commercial microscopes clinically/medically approved for their use on humans exist, in either tabletop (DermaInspect™, since 2002) or in a more flexible, compact and "portable" configuration (MPT*flex*™, since 2011) more suitable for clinical use [45]. The clinical applications of *in vivo* multiphoton/FLIM microscopy range from the characterization of age-related or photoaging changes [38, 46–55]], dermatological disorders and melanoma [28, 56–71], up to the assessment of penetration and effects of pharmaceutical/cosmetic products on human skin [19, 21, 55, 72–81].

19.2 Clinical multiphoton FLIM systems

Two types of multiphoton FLIM microscopes classified as class 1M devices, medically approved by certified bodies of the European Union for their use on humans are nowadays commercially available (JenLab GmbH, Germany).

The first system on the market was the DermaInspect™ in 2002 [6], a tabletop microscope that offers high quality simultaneous 2PEF and SHG imaging of epidermis and superficial dermis up to a depth of about 160–200 µm depending on the body region [19]. It also enables fluorescence lifetime imaging that is performed using a time-correlated single-photon counting (TCSPC) unit (SPC830 from Becker & Hickl GmbH, Berlin, Germany). Most of the clinical trials performed with this system were done on the forearm. Within this region, good signal-to-noise ratio images can be acquired up to a depth of 160 µm with an average excitation power increasing from 10 mW at the skin surface up to 50 mW when reaching the dermis [19]. The excitation wavelength can also be varied as this system is equipped with tunable femtosecond pulsed lasers, but an optimal excitation of a maximum of endogenous fluorophores is obtained when working at wavelengths around 760 nm [5]. This excitation wavelength also enables second harmonic generation, as this signal is generated at exactly half the excitation wavelength ($\lambda/2$). An example of a z-stack of 2PEF/SHG images acquired on normal human forearm skin can be found in [19] and images acquired at different depths are given in Fig. 19.1.

In the epidermis, typically, the first 10 µm reveal the organization of the *stratum corneum disjunctum* – SCD (made of corneocytes – polygonal-shaped dead keratinocytes emitting a 2PEF signal that mainly arises from keratin) and the next 10 µm correspond to *stratum corneum compactum* – SCC (this epidermal layer creates less intense 2PEF signals and presents an almost homogenously distributed pattern with no distinguishable cell structures). The presence of cell nuclei indicates the tran-

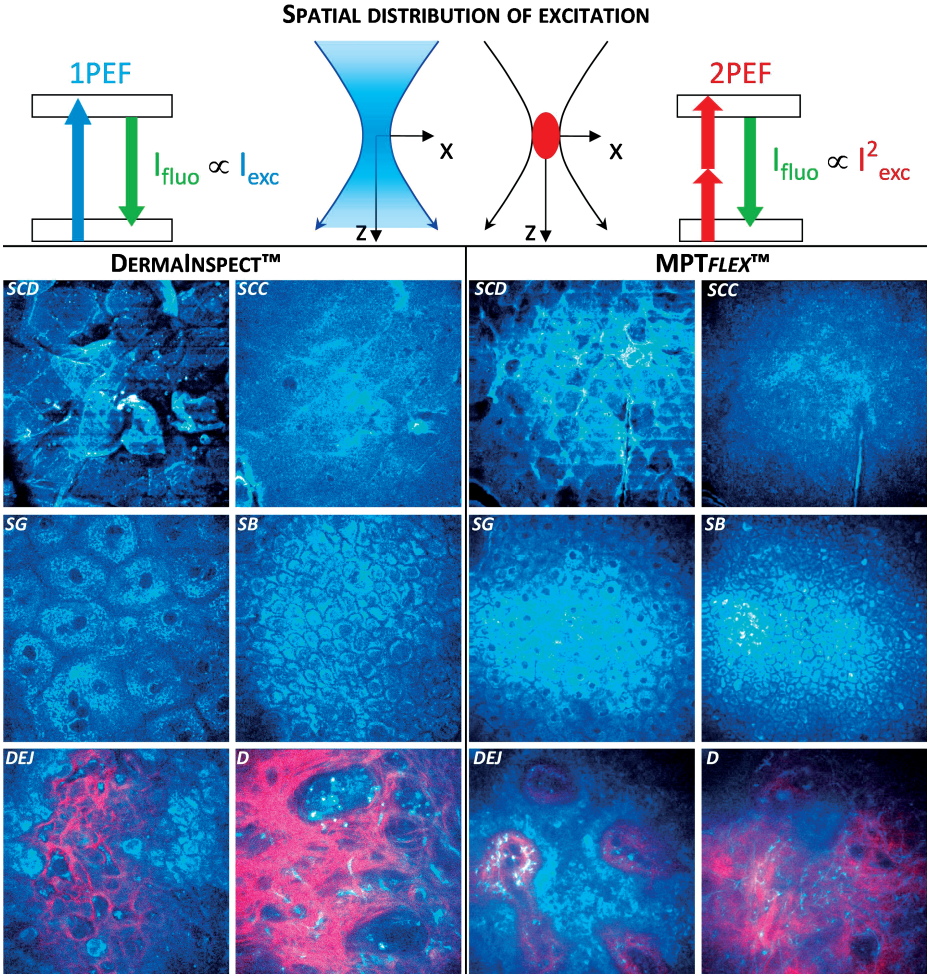

Fig. 19.1: (Top) Spatial distribution of illumination in one-photon and two-photon excitation process. (Bottom) Example of multiphoton 2PEF/SHG images acquired *in vivo* on human skin forearm with the DermaInspect™ and MPT*flex*™ systems at different depths. 2PEF signal (cyan hot color) reveals the endogenous fluorophores distribution inside the epidermis and dermis (elastic fibers, fibroblasts) whereas the SHG signal (red color) reveals the collagen fibers. Acquisition conditions: DermaInspect™ – 511 × 511 pixels, 0.255 µm/pixel; 130 × 130 µm^2, 7.4 s/image; MPT*flex*™ – 511 × 511 pixels, 0.4 µm/pixel; 205 × 205 µm^2, 4.4 s/image.

sition to living epidermis (*stratum granulosum, spinosum* and *basale*). The living cells, mainly keratinocytes, show homogenous fluorescent cytoplasm and nonfluorescent membranes and nuclei. Their diameter is about 30 µm in *stratum granulosum* and reaches 10 µm in *stratum basale* (both cell diameter and the ratio between the cytoplasmic and nuclear volumes decrease with depth). The cytoplasm fluorescence of the epidermal living cells is mainly due to mitochondrial NADH upon ≈ 760 nm excitation.

A 2PEF signal is also detected from melanin, which is found in different concentrations within some epidermal cells and mainly in the basal layers of the epidermis. As previously mentioned, a highly intense 2PEF signal, greater than the one created by the other cellular fluorophores, can be obtained in the basal layers where melanin is highly concentrated. FLIM can help distinguishing the less concentrated melanin regions inside the epidermis presenting comparable fluorescence intensities with the other cytoplasmic fluorophores. But, unfortunately, 2PEF-FLIM imaging does not allow distinguishing keratinocytes from melanocytes or from other epidermal cells such as Langerhans cells. Melanocytes can only be identified *in vivo* by multiphoton imaging in diseases such as melanoma due to the abnormal melanin accumulation in these cells and especially into their dendrites [58].

In the dermis, SHG and 2PEF contrast modes offer an insight into the 3D structure of superficial dermis (≈ 100 µm). In young volunteers, this region corresponds to the papillary dermis, but in older volunteers, the superficial part of the reticular dermis can also be imaged (due to epidermal atrophy with age, flattening of the dermal-epidermal junction and thinning of the papillary dermis).

In multiphoton images, the interface between the epidermis and dermis is revealed by the appearance of an SHG signal. This signal is created by the fibrillar collagens and allows visualizing the collagen fiber organization inside the dermal papilla. The other visible constituents are the elastic fibers, the dermal cells (probably fibroblasts), the blood capillaries and blood cells often seen inside these capillaries.

In clinical trials, one needs to acquire several z-stacks of multiphoton images in different regions of an area of interest. In practice, in our clinical trials, we limited the measures to a minimum of 2 acquisitions as 3D imaging is time consuming. Typically, with the DermaInspect™, a multiphoton 3D (x, y, z) image of $130 \times 130 \times 162\,\mu m^3$ volume, corresponding to a z-stack of 70 *en face* images, can be acquired in less than 10 minutes (z-stack of 511 × 511 pixels images with 0.255 µm/pixel acquired every 2.35 µm; 7.4 s/image). But almost an hour per two areas of interest is starting to become tiring for the volunteers, not to mention the additional time required for image reacquisition, in case the volunteer moved during the acquisition. Hopefully, technology evolves and the new MPT*flex*™ system overcomes this difficulty by employing more sensitive detectors which offer the possibility of reducing the pixel dwell time.

MPT*flex*™, a second generation CE-marked, medically-certified multiphoton FLIM microscope available since 2011, presents several advantages over the DermaInspect™ [45]. First of all, it is a compact and therefore easily transportable system. It benefits from improved ergonomics due to the flexible articulated mechano-optical arm that opens the way to an *in vivo* investigation of human body areas less accessible such as face, scalp and armpits. The detection efficiency has been improved with the use of more sensitive detectors, but also by their implementation in a "miniaturized" scanning head at the end of the articulated arm. When comparing images acquired with similar pixel dwell times, the MPT*flex*™ offers an increased imaging depth even though the excitation power is limited to a maximum of 30 mW. The field of view is

≈ 4 times higher reaching $250 \times 250\,\mu m^2$ (see Fig. 19.1) and wide-field images can also be acquired within a $5 \times 5\,mm^2$ region by mosaic scanning using the motorized scan head. In practice, to keep a reasonable image acquisition time per z-stack, one has to reduce the FOV and/or the pixel dwell time. A z-stack of $205 \times 205 \times 162\,\mu m^3$ (65 *en face* 511×511 pixels images, $dx = 0.4\,\mu m$, $dz = 2.54\,\mu m$; 4.4 s/image, 16.8 µs/pixel) can be acquired in less than 5 minutes.

19.3 Quantitative data afforded by multiphoton imaging of human skin *in vivo*

The routine use of multiphoton microscopy in clinical practice requires specific automated image processing tools that would allow the investigator to extract pertinent quantitative 3D-information on skin layers and constituents. Up to now, very few image processing methods have been developed for characterizing multiphoton images of human skin *in vivo*. In the dermis, the proposed methods are mainly based on the computation of the mean intensity of 2PEF and SHG signals, or of the density of pixels occupied by these signals on conveniently chosen 2D slices within dermis at a fixed depth from the skin surface [46–49]. Parameters linked to the epidermis thickness [32] and keratinocytes morphology estimated on 2D slices within granulosum and spinosum layers [65] have also been proposed. But neither of these parameters was assessed in the 3D epidermal or dermal volume.

In the past years, our team focused on segmenting the multiphoton images in order to automatically separate the epidermis from the dermis [38] and validating 3D quantification parameters of interest for the study of photoaging or whitening phenomena [19–21, 50]. We developed a user-friendly software, the Multiphoton Skin Tools Suite (MPSTS), allowing to choose a set of 3D acquisitions, build the list of measures to compute and run a batch processing to compute all the segmentations as well as the measures for an entire clinical study. The tools that we propose open the possibility of characterizing in 3D the skin layers and sublayers, the cells, their melanin content or the elastic and collagen fibers in terms of quantity, size and organization.

19.3.1 Automatic 3D segmentation of skin layers

The aim of the segmentation is to classify each image voxel in one of the following compartments: coupling medium (CM), epidermis (ED) or dermis (D). Such a task is all but trivial, especially if the dermal-epidermal junction (DEJ) is neither flat nor parallel to the image plane. Moreover, given that a typical multiphoton clinical study may contain several hundred stacks of images, the segmentation method should not be time consuming. From a methodological image processing viewpoint, the main difficulties encountered with multiphoton skin images are:

- The signal tends to be more intense near the optical axis and decreases with the imaging depth, due to attenuation and diffusion of excitation and emission light.
- The SHG signal is specific to the dermis, but not enough to delimit it, as at the DEJ level, dermal regions can be found with elastic fibers only and no collagen fibers, *i.e.*, an absence of SHG signal.
- The sampling steps are not isotropic and the vertical resolution and sampling steps are large with respect to some structures, such as cells at the top of the living epidermis.

To overcome these difficulties, we use a marker-based approach. The general strategy is summed up by the flow chart shown in Fig. 19.2. Markers, sets of pixels considered as specific to a compartment, are afterwards propagated to the entire image volume, in order to have a complete partition.

The propagation is done in two steps:

(i) a fast watershed algorithm produces a low-level segmentation, made of super-voxels (small, homogeneous regions);
(ii) the super-voxels are merged, taking into account the markers, thanks to a graph cut algorithm.

All processing is done in 3D, except when otherwise specified. Moreover, the current version of the segmentation method, which has not undergone any specific computational optimization, takes an average of one minute to process a 3D multiphoton image on a classical personal computer (Intel core i7, 8 GB memory). For details, we refer the reader to [38].

At this stage, an epidermis mask, *i.e.*, a 3D binary image corresponding to the epidermis compartment is available for further processing. Using modern mathematical morphology operators, it is possible to further segment the epidermal layers, namely *stratum corneum* (SC) and *living epidermis* (LED). This automatic segmentation method allows quantifying independently the different compartments inside the epidermis (see Fig. 19.2). Moreover, a more refined segmentation of the epidermis can also be calculated: by defining 12 normalized layers inside the epidermis, one can have access, for example, at the melanin density distribution along the z-axis inside the epidermis.

19.3.2 Pseudo-FLIM specific melanin detection

So far, available melanin detection methods lacked specificity, were limited to 2 dimensions and/or needed invasive biopsies. The classical assessment method is based on Fontana–Masson histological staining associated with 2D white light imaging. But this approach is invasive and inappropriate in clinical studies where follow-up

of melanin changes is needed. Confocal microscopy enables a non-invasive melanin visualization based on its higher reflectivity, but cellular membranes and corneocytes exhibit similar reflection signals, making melanin detection and quantification impossible.

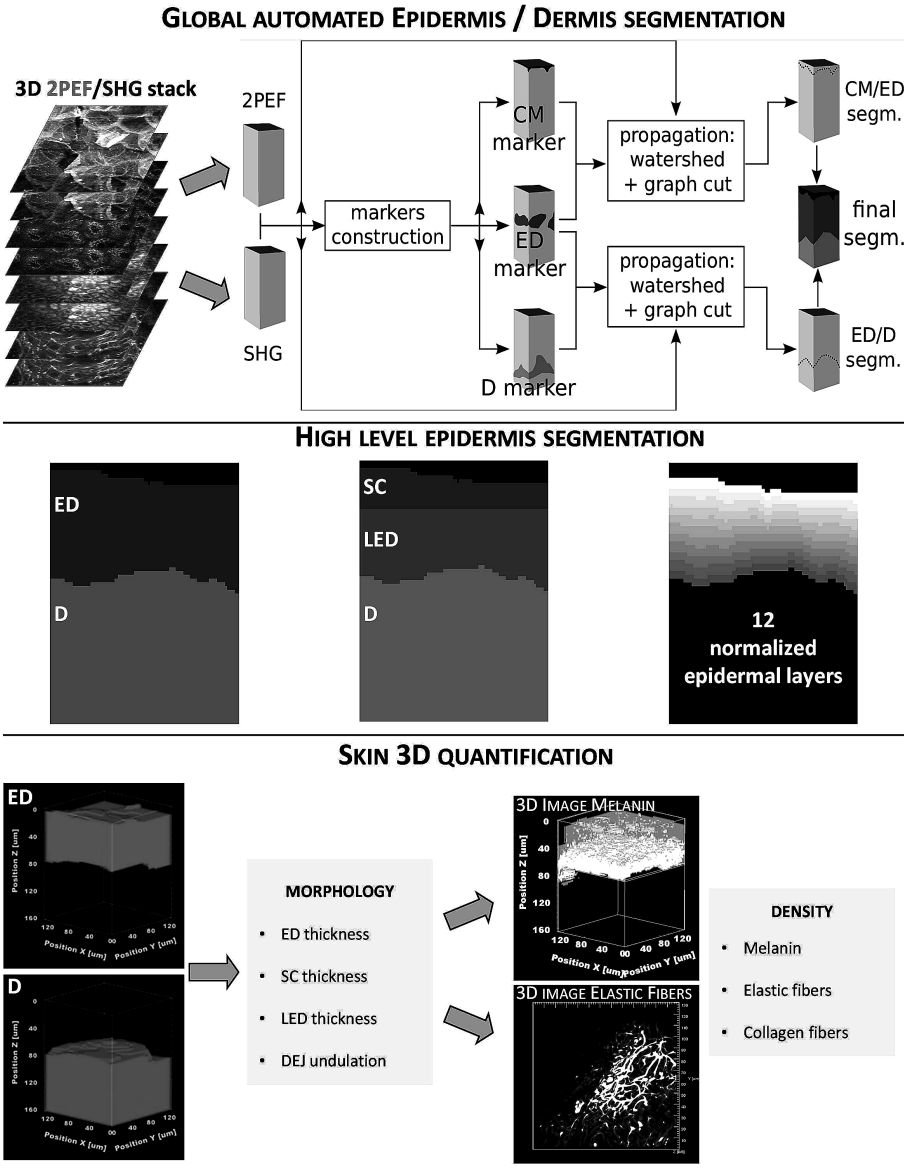

Fig. 19.2: General automated segmentation and quantification strategy for *in vivo* multiphoton FLIM images of human skin implemented in the MPSTS software.

In multiphoton microscopy, melanin quantification based on the 2PEF signal intensity can be performed in the basal layers of epidermis, where melanin is often highly concentrated [19]. But methods based upon fluorescence intensity levels are not always satisfactory: high 2PEF signals can also be detected from other fluorophores (e.g., keratin in the *stratum corneum*), and regions with low melanin concentration (low intensities) will not be taken into account.

FLIM affords specific melanin detection based on its lifetime, but the long acquisition times are incompatible with 3D imaging on human volunteers. In practice it is limited to selected 2D slices at a depth chosen by the user.

We proposed another approach based on multiphoton FLIM, called Pseudo-FLIM, to specifically detect melanin in the whole epidermis [20]. This requires binning the fluorescence photons in a reduced number of time channels (4 instead of 256, 2 ns/time channel). This can be done either at the acquisition or afterwards during processing. In our studies, we use the first option (see Fig. 19.3). The main steps are:

(i) apply a 2D-Gaussian filter on the raw 4-time channels images;
(ii) calculate a log linear regression on the first 3-time channels for each (x, y) pixel;
(iii) calculate a slope parametric image;
(iv) create a melanin mask by applying a threshold that keeps only the high slope values.

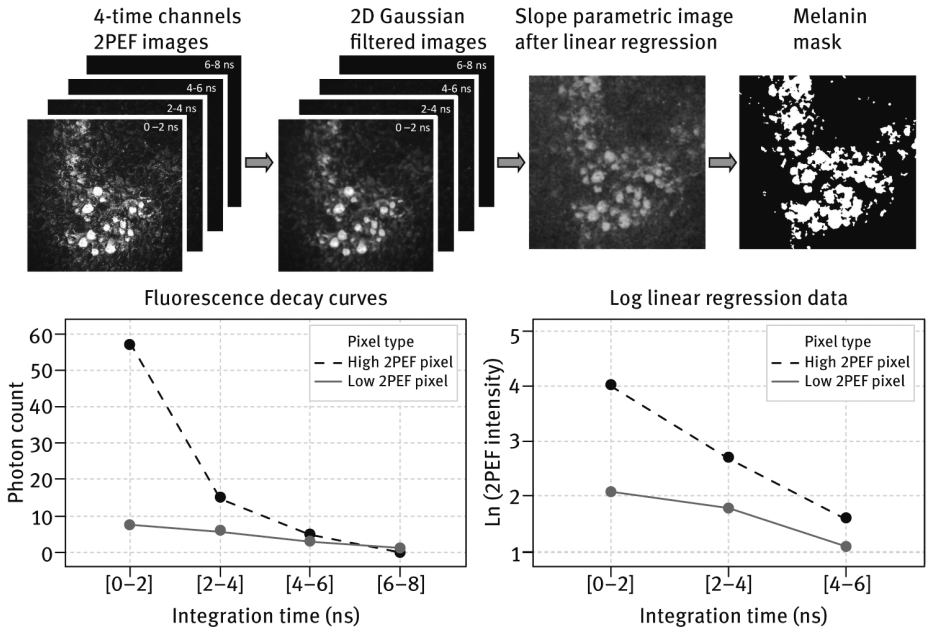

Fig. 19.3: Pseudo-FLIM Melanin quantification process. Specific melanin detection is done using an approach, called Pseudo-FLIM, which allows detecting melanin from multiphoton FLIM-like data compatible with 3D *in vivo* acquisitions on human volunteers as only a few photons per pixels are needed.

The slope of the decay (the higher the slope, the shorter the lifetime) allows to identify melanin pixels, as melanin presents a very short ($\tau_1 < 0.1$ ns) and predominant ($a_1 > 90\,\%$) lifetime component (i.e., high slope values). As this analysis requires only a few photons per pixel, it results in a short image acquisition time (≈ 30 photons per pixel; $\approx 16\,\mu$s pixel dwell time) compatible with 3D imaging on humans.

19.3.3 Quantitative parameters

The 3D automatic segmentation opens the possibility of automatically computing quantitative measurements, on the segmentation frontiers (skin surface and DEJ), and within each layer (ED, SC, LED, D). Each measure is generically defined as the combination of a modality, a region of interest and an operator. Modalities are, for example, 2PEF, SHG or Pseudo-FLIM. Regions of interest (ROI) can be layers such as the dermis or epidermis, but also frontiers such as the DEJ. Operators compute the final measure using the modality and the ROI. For example, by choosing 2PEF as modality, ED as ROI, and the mean operator, one can compute the mean value of 2PEF intensity within the epidermis. We classify the quantitative parameters extracted from skin multiphoton images into morphological and density measures (see Fig. 19.2) [38].

19.3.3.1 Morphological measures

Morphological measures characterize the regions and frontiers shapes. They are directly derived from the 3D segmentation, without further need of the raw multiphoton signals. One can, for example, estimate the thickness (T) of the living epidermis in µm, T(LED), by calculating it along the z-axis at each (x, y) position and computing its mean value. It is also possible to quantify the DEJ undulation by estimating its normalized area, NA(DEJ), defined as the ratio between the areas of the DEJ surface and its projection on a horizontal plane. A value of 1 implies a totally flat and horizontal DEJ and higher values indicate a more undulated DEJ.

19.3.3.2 Density measures

The density measures can be estimated in 3D in the whole epidermal and dermal layers and sublayers. They aim at characterizing the melanin density in the epidermis or the elastic and collagen fiber density in the superficial dermis. The density parameter requires a binary mask computed by applying a threshold to 2PEF, SHG or Pseudo-FLIM modalities in order to detect the pixels containing melanin, elastic or collagen fibers. It is defined as the ratio of voxels occupied by these constituents to the total number of voxels of the ROI onto which the density is estimated. We also compute in the whole 3D imaged superficial dermis the SHG-to-AF aging index of dermis (3D–SAAID (D)), which has only been calculated in 2D in the literature [46, 82].

19.4 Cosmetic applications

The domain of application is dictated by the type of endogenous signals/constituents that can be evidenced by multiphoton FLIM microscopy. Cosmetic applications range from knowledge to evaluation studies aiming to acquire a better knowledge of skin differences appearing with aging, UV or solar exposure or between the different skin phototypes, as well as to evaluate the efficacy of cosmetic anti-aging or whitening ingredients. The penetration of cosmetic compounds could also be investigated by multiphoton FLIM techniques provided that their 2PEF emission spectrum and/or fluorescence lifetime are different compared to the ones of endogenous skin constituents.

In the following, we will discuss the most straightforward cosmetic clinical applications. The clinical trials described hereafter were performed with the DermaInspect™ device. The experimental protocols were approved by the Saint Louis Hospital ethics committee, complying with the Declaration of Helsinki. All volunteers gave written, informed consent.

19.4.1 Photo-aging

The study of age-induced skin modifications with multiphoton FLIM microscopy is of particular importance if one wants to non-invasively assess the anti-aging effects of a cosmetic compound at the microscopic level and follow these effects over time, before and after product application. To explore the 3D skin differences that can be evidenced by multiphoton microscopy, we performed a clinical trial on 15 young (18–25 a) and 15 aged (70–75 a) Caucasian human female volunteers, focusing on ventral and dorsal forearm sides (sun protected vs. sun-exposed) [38, 50].

As previously mentioned, with multiphoton microscopy epidermis and superficial dermis can be characterized in 3D up to a depth of approximately 160 µm. In young subjects, dermis includes papillary dermis and a limited fraction of reticular dermis, whereas in elderly subjects it mainly corresponds to reticular dermis as defined in histology due to epidermis atrophy and loss of DEJ undulation. In spite of the very limited field of view and imaging depth, as compared to histology, multiphoton imaging and image processing provide quantitative parameters in agreement with what is known for skin aging and photoaging, without the need for skin biopsy.

The 3D quantification data on epidermal thickness and DEJ undulation are shown in Fig. 19.4. We observed no difference in mean thickness of the epidermis between dorsal and volar side of the forearm, but a decrease with age, in agreement with the literature.

Similarly, the normalized area of the dermal-epidermal junction, which is related to the shape of the DEJ, decreases with age without any differences between dorsal and volar side. As expected, with age the ridges of the DEJ flatten out. The melanin content

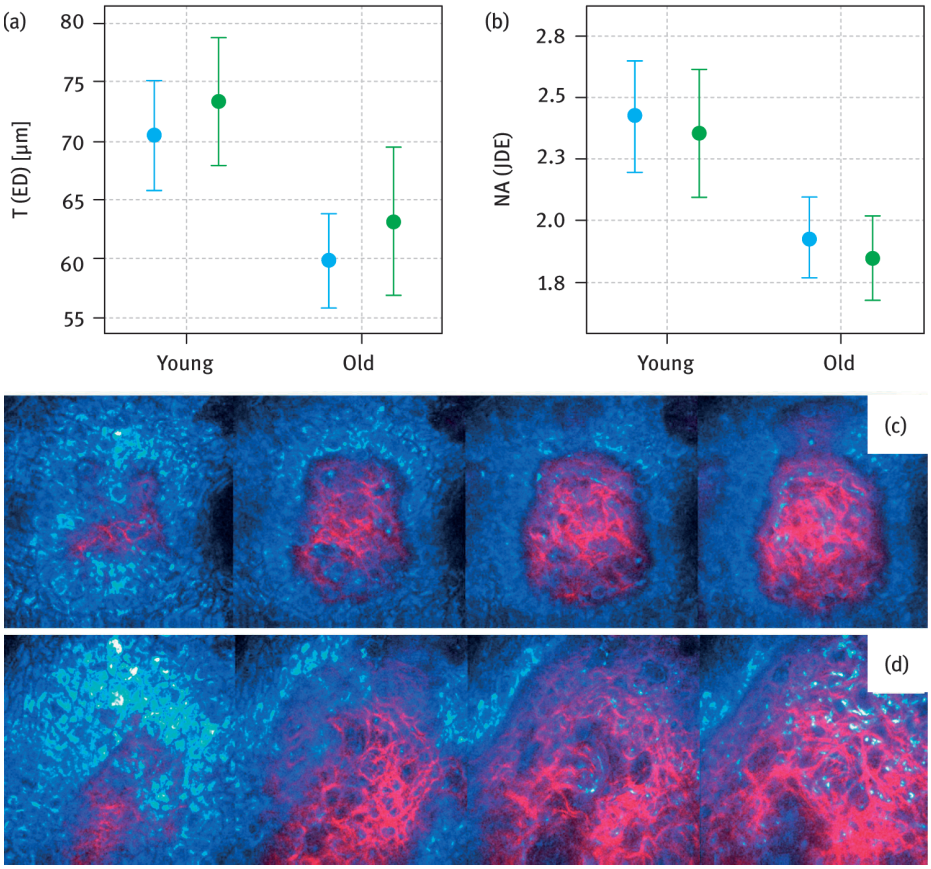

Fig. 19.4: Epidermal changes induced with photo-aging: (a) epidermal thickness; (b) normalized area of DEJ. The 2PEF/SHG images (ventral forearm side) give insights into the shape of the DEJ: round papillae in young volunteers, and flattened ones in old volunteers (d). For each age class, the left blue bars correspond to the ventral measures, and the right green ones to the dorsal measures. Error bars correspond to 95 % confidence intervals of the mean.

(data not shown) is higher on dorsal versus volar side of the forearm, but without any difference between young and old volunteers.

Fig. 19.5 shows the changes occurring with age in the superficial dermis, namely the changes in the elastic and collagen fiber densities that can be evidenced with multiphoton microscopy.

For the mean density of elastic fibers, 3D-2PEF Density (D), an increase is observed with age due to solar elastosis and no differences between dorsal and ventral forearm sides. The mean density of collagen fibers, 3D-SHG Density (D), shows no difference between young and old groups, but is higher on ventral sides compared to dorsal ones.

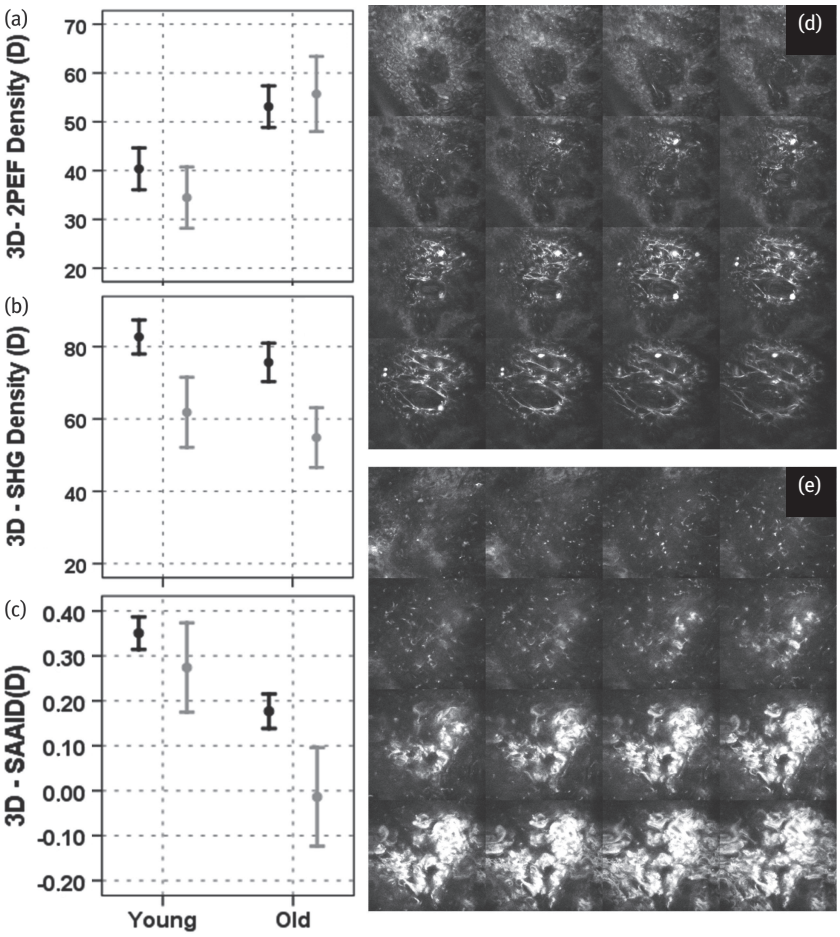

Fig. 19.5: Dermal changes induced with photo-aging in the 3D density of (a) elastic fibers and (b) collagen fibers. The two densities can be used to calculate in 3D the SHG-to-AF aging index of dermis – 3D-SAAID (c). The 2PEF images (dorsal forearm side) show the elastic fibers differences between (d) young and (e) old volunteers. The increase in elastic fiber density with age, due to solar elastosis, is clearly seen (e). For each age class, the left black bars correspond to the ventral measures, and the right gray ones to the dorsal measures. Error bars correspond to 95 % confidence intervals of the mean.

The SHG-to-AF aging index of dermis 3D-SAAID (D), estimated here in the whole imaged volume of superficial dermis, highly decreases with age as also evidenced in 2D at a fixed depth from the skin surface [46, 82]. Moreover, its mean value is also lower on the sun-exposed dorsal forearms compared with the sun-protected ventral side. Negative values mean that there are more significant pixels with 2PEF than with SHG signals, and a value close to zero means that both proportions are similar.

The changes with age in the elastic and collagen fibers can also be addressed in terms of organization, by quantifying the relative position of 2PEF and SHG signals [38].

The estimation of all these density-based measures is more representative of the superficial dermis in 3D than in 2D. The 2D measurements of elastic or collagen fiber density done at a specific fixed imaging depth can be impacted, for example, by the changes in epidermis thickness or DEJ undulation. This is problematic when one wants to assess the effects of cosmetic products or any other effects, especially if the morphology of the epidermis is also modified. In this case, at a fixed depth from the skin surface, the variations in elastic or collagen fiber densities cannot be attributed to the product alone, as the dermal regions investigated before and after product application will not be the same. Not only does the 3D approach avoid the selection of a 2D plane, but the measurements are based on a larger, more representative, volume of tissue. The density measurements are also more robust than the intensity measurements, as these are directly dependent on the excitation power. The excitation power delivered at a certain depth will depend upon epidermal thickness, the presence of melanin or other constituents that can attenuate or diffuse both the laser and the emitted multiphoton signals. More generally, the interpretation of a quantitative parameter should be done by taking into account all the available information in a study.

With this photo-aging study, we showed for the first time that it is possible to process and extract in 3D quantitative measurements revealing expected aging effects.

19.4.2 Study of constitutive pigmentation

Melanin-specific detection by multiphoton FLIM opens the possibility to non-invasively characterize the changes between the different skin phototypes, the pigmentation disorders or to assess compounds able to modulate skin melanin content. When combining the Pseudo-FLIM specific melanin detection with the high level segmentation of the epidermis, one can not only have non-invasive access to the global melanin density, but also to its z-distribution through the epidermis.

In a clinical trial on 45 female volunteers (18–55 a) with different skin color (Individual Typology Angle [83] – ITA values of their ventral forearm ranging from very light – grade I to brown skin – grade V), we evidenced an increase in the global mean melanin density with ITA group, as expected and in agreement with histology (see Fig. 19.6). Moreover, we studied the melanin density normalized z-profile from the dermal-epidermal junction up to the *stratum corneum*. Our results show an increased melanin density at the basal layers for ITA groups II to V, almost no differences at the level of *stratum granulosum* and a slight increase in melanin density at the level of *stratum corneum* for darker skin color.

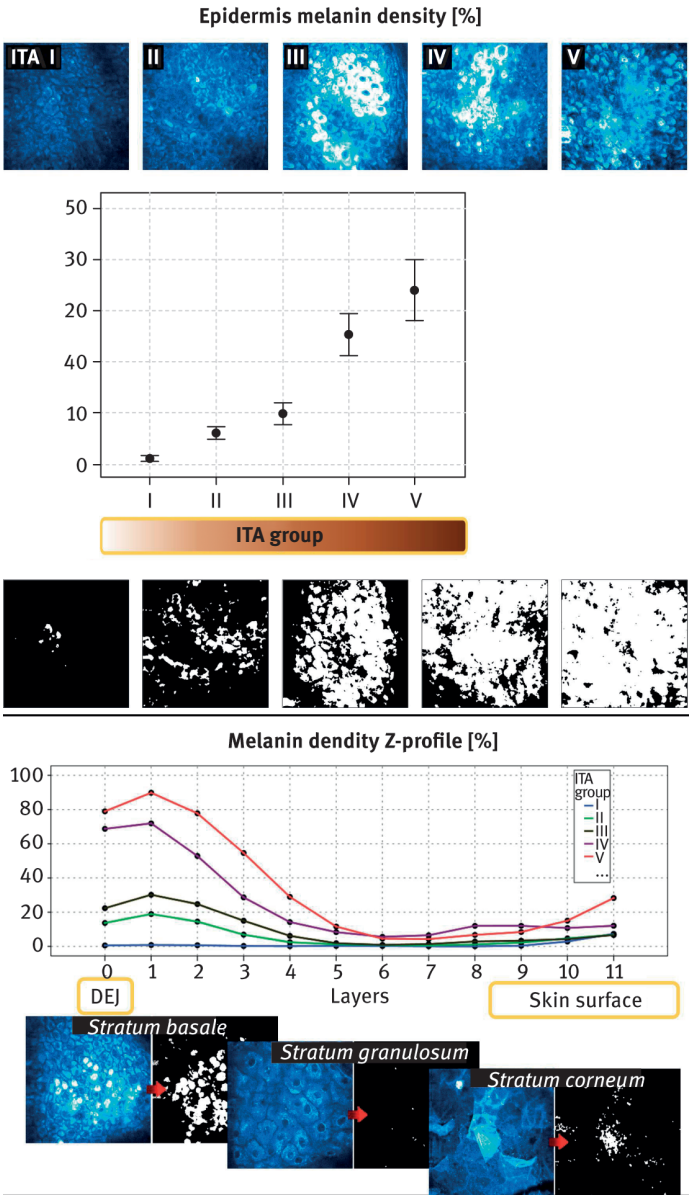

Fig. 19.6: Change with skin color in (top) mean global melanin density of the epidermis and (bottom) in the normalized melanin density *z*-profile (12 normalized layers from 0 – DEJ level to 11 – SC level). The data are expressed in % and error bars correspond to 95 % confidence intervals of the mean. Raw 2PEF images are shown in cyan hot color and melanin masks images obtained by Pseudo-FLIM method in white color.

This innovative approach could have large applications in both the dermatological and cosmetic fields, since easily applied to the characterization of pigmentation disorders or to the assessment of compounds able to modulate skin melanin content.

19.4.3 Efficacy assessment of anti-aging or whitening cosmetic ingredients

Multiphoton FLIM microscopy, as shown above, is able to evidence the age-induced skin changes and the differences in constitutive pigmentation. One of the most straightforward applications in cosmetics is the overtime follow up of the efficacy of anti-aging and whitening ingredients. This can be done in either long-term studies in which the products are applied for weeks or months or in short-term studies during about one month. The ability of multiphoton microscopy to continuously monitor and evaluate epidermal effects of pharmaceutics compounds in short-term study is shown in [19].

In the following, we will give an example of efficacy evaluation of anti-photoaging agents in a short-term screening protocol based on an occlusive patch test. The occlusive patch test was initially developed for assessing topical retinoid activity in human skin and has been extended as a short-term screening protocol for anti-aging agents. In this model, biopsies are performed at the end of the occlusion period for morphological and immunohistochemistry analysis. Our main objective with this study was firstly, to demonstrate that multiphoton microscopy, in association with a patch test, could be used as a short-term screening protocol for anti-aging and whitening agents, and secondly, to validate the relevance of this method for kinetic and quantitative assessment with gold standards of anti-aging that are retinoids.

For that, 20 women, aged 50–65 years, were enrolled. Retinol 0.3 % (RO) and Retinoic acid 0.025 % (RA) were applied to the dorsal photodamaged side of their forearm under occlusive patches for 12 days. A patch alone was applied to a third area as control. Evaluation was performed at day D0, D12 (end of treatment), D18 and D32 using multiphoton microscopy. Epidermal thickness, normalized area of the DEJ and melanin density were estimated using the 3D image processing tools described in Section 19.3. Both RO and RA induced changes in these 3 parameters (see the complete study results in [21]). The anti-aging (epidermal thickening, increase in DEJ undulation) and whitening (decrease in melanin density) effects of RO are shown in Fig. 19.7.

Retinol induced an epidermal thickening due to living epidermis thickening with no effect on SC. This effect was significant at D12 (end of the treatment), D18 and D32 vs. baseline and vs. control.

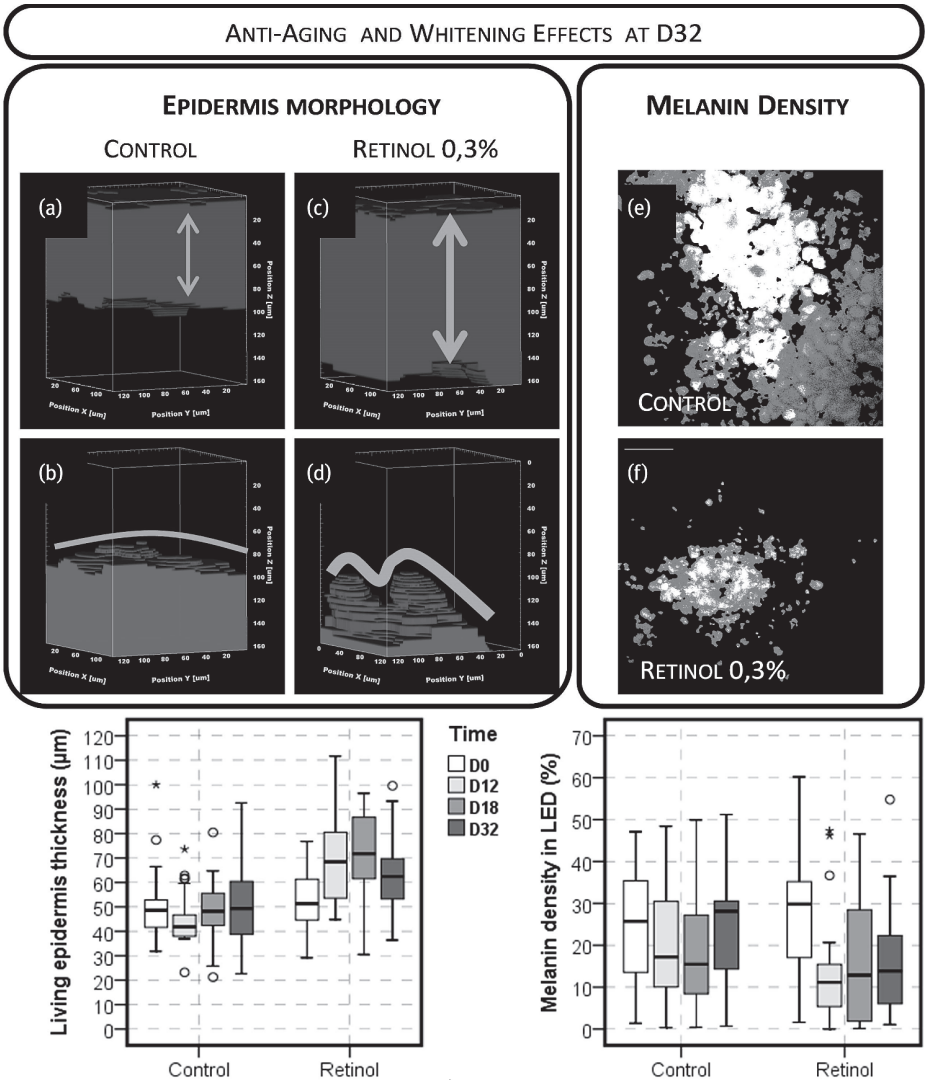

Fig. 19.7: Quantification results of Retinol effects obtained with multiphoton microscopy. The epidermal thickening and the increase in DEJ undulation at D32 for control and Retinol 0.3 % can be visualized on the 3D volume renderings of the segmented epidermal (a, c) and dermal (b, d) compartments. Images (e) and (f) acquired at the basal layers exemplify the melanin density changes. The 3D quantification data are expressed as boxplots with fences. The boxes contain 50 % of the data; the intervals between the lower limit of the box and the lower inner fence contain 25 %, and vice versa for the other 25 %. — indicates the median that divides the population in two groups with equal numbers of data points; ° the outliers and * the extreme data points.

Additionally, multiphoton microscopy evidenced an increase in DEJ undulation with retinoid treatment, the effect of retinol being, to our knowledge, a new finding.

Retinoid-induced decrease in melanin content is also observed for the first time in such a short-term protocol. In some subjects, visible skin whitening was observed on retinoid-treated areas which correlate with the decrease in melanin density. Changes in melanin density are clearly visible on melanin masks obtained using Pseudo-FLIM specific melanin detection method (Fig. 19.7 (e) and (f)).

Dermal changes could not be addressed in this study, in which epidermal thickness increased drastically and exceeded the imaging depth at some time points. We believe that cosmetic product-induced dermal changes that could be addressed with multiphoton microscopy are not likely to be observed in such a short 12 days period of treatment. Possible effects in the superficial dermal structure using this technique should be addressed in long-term studies with open applications.

This study shows that short-term protocol in combination with non-invasive *in vivo* multiphoton microscopy allows epidermal effects induced by retinoids, including melanin content, to be accurately detected and quantified over time. This is the first application of innovative specific 3D quantification tools for multiphoton images to the evaluation of a cutaneous treatment.

19.5 Conclusion

Multiphoton FLIM in cosmetic clinical research is an exciting area of application of this innovative and non-invasive imaging tool, compatible with *in vivo* studies on human volunteers. In association with specific 3D image processing, one can extract several representative quantitative parameters characterizing skin constituents in terms of morphology, density and organization in both epidermis and superficial dermis. In spite of the very limited field of view and imaging depth, as compared to histology, multiphoton FLIM imaging and image processing provide quantitative data of interest in skin photo-aging and pigmentation, without the need for skin biopsy. These innovative approaches opened the way to the kinetic evaluation of the efficacy of cosmetic molecules at the subcellular level. With the arrival of flexible and compact imaging systems, future work in this domain will focus on human face skin, the preferred body region for the application of cosmetic products.

References

[1] Wilhelm KP, Elsner P, Berardesca E, Maibach HI. Bioengineering of the skin: skin imaging and analysis. 2nd edition. New York: Informa Healthcare USA Inc.; 2007.

[2] Masters BR, So PTC, Gratton E. Multiphoton excitation fluorescence microscopy and spectroscopy of in vivo human skin. Biophysical Journal. 1997;72:2405–2412.

[3] Teuchner K, Freyer W, Leupold D, Volkmer A, Birch DJS, Altmeyer P, Stucker M, Hoffmann K. Femtosecond two-photon excited fluorescence of melanin. Photochemistry & Photobiology. 1999;70:146–151.
[4] Campagnola PJ, Millard AC, Terasaki M, Hoppe PE, Malone CJ, Mohler WA. Three-dimensional high-resolution second-harmonic generation imaging of endogenous structural proteins in biological tissues. Biophysical Journal. 2002;82:493–508.
[5] Zipfel WR, Williams RM, Christiet R, Nikitin AY, Hyman BT, Webb WW. Live tissue intrinsic emission microscopy using multiphoton-excited native fluorescence and second harmonic generation. Proceedings of the National Academy of Sciences of the United States of America. 2003;100:7075–7080.
[6] König K, Riemann I. High-resolution multiphoton tomography of human skin with subcellular spatial resolution and picosecond time resolution. Journal of Biomedical Optics. 2003; 8:432–439.
[7] Pena AM, Strupler M, Boulesteix T, Godeau G, Schanne-Klein MC. Spectroscopic analysis of keratin endogenous signal for skin multiphoton microscopy. Opt Express. 2005;13:6268–6274. Erratum 13(17):6667.
[8] König K. Multiphoton microscopy in life sciences. Journal of Microscopy. 2000;200:83–104.
[9] Zipfel WR, Williams RM, Webb WW. Nonlinear magic: multiphoton microscopy in the biosciences. Nature Biotechnology. 2003;21:1369–1377.
[10] Göppert-Mayer M. Über Elementarakte mit zwei Quantensprüngen. Annalen der Physik. 1931; 401:273–294.
[11] Grzybowski A, Pietrzak K. Maria Goeppert-Mayer (1906–1972): Two-photon effect on dermatology. Clinics in Dermatology. 2013;31:221–225.
[12] Kaiser W, Garrett CGB. Two-photon excitation in CaF2: Eu2+. Physical Review Letters. 1961;7: 229–231.
[13] Denk W, Strickler JH, Webb WW. Two-photon laser scanning microscopy. Science. 1990;248: 73–76.
[14] Pena AM, Boulesteix T, Dartigalongue T, Schanne-Klein MC. Chiroptical effects in the second harmonic signal of collagens I and IV. J Am Chem Soc. 2005;127:10314–10322.
[15] Periasamy A, Clegg RM. FLIM microscopy in biology and medicine. 1st edition. Boca Raton, Florida: Chapman and Hall/CRC, Taylor & Francis Group; 2010.
[16] Dancik Y, Favre A, Loy CJ, Zvyagin AV, Roberts MS. Errata: Use of multiphoton tomography and fluorescence lifetime imaging to investigate skin pigmentation in vivo. Journal of Biomedical Optics. 2013;18:029802.
[17] Chance B, Estabrook RW, Ghosh A. Damped sinusoidal oscillations of cytoplasmic reduced pyridine. Proceedings of the National Academy of Sciences of the United States of America. 1964;51:1244–1251.
[18] Georgakoudi I, Quinn KP. Optical imaging using endogenous contrast to assess metabolic state. Annual Review of Biomedical Engineering. 2012;14:351–367.
[19] Ait El Madani H, Tancrède-Bohin E, Bensussan A, Colonna A, Dupuy A, Bagot M, Pena AM. In vivo multiphoton imaging of human skin: assessment of topical corticosteroid-induced epidermis atrophy and depigmentation. Journal of Biomedical Optics. 2012;17:026009.
[20] Pena AM, Baldeweck T, Tancrede E, Decencière E, Koudoro S, inventors; Non-invasive method for specific 3D detection, visualization and/or quantification of an endogenous fluorophore such as melanin in a biological tissue. France patent FR2982369. International publication number WO2013068943; 2011.
[21] Tancrède-Bohin E, Baldeweck T, Decencière E, Brizion S, Victorin S, Parent N, Faugere J, Souverain L, Bagot M, Pena AM. Non-invasive short-term assessment of retinoids effects on human

skin in vivo using multiphoton microscopy. Journal of the European Academy of Dermatology and Venereology. 2015;29:673–681.
[22] Masters BR, So PTC, Gratton E. Optical biopsy of in vivo human skin: Multi-photon excitation microscopy. Lasers in Medical Science. 1998;13:196–203.
[23] Masters BR, So PTC, Gratton ENRI. Multiphoton Excitation Microscopy of In Vivo Human Skin: Functional and Morphological Optical Biopsy Based on Three-Dimensional Imaging, Lifetime Measurements and Fluorescence Spectroscopy. Annals of the New York Academy of Sciences. 1998;838:58–67.
[24] Masters BR, So PTC. Multi-photon excitation microscopy and confocal microscopy imaging of in vivo human skin: A comparison. Microscopy and Microanalysis. 1999;5:282–289.
[25] Masters BR, So PTC. Multiphoton excitation microscopy of human skin in vivo: Early development of an optical biopsy. Proc SPIE 4001; 2000. p. 156–164.
[26] Masters BR, So PTC. Confocal microscopy and multi-photon excitation microscopy of human skin in vivo. Optics Express. 2001;8:2–10.
[27] König K, Ehlers A, Riemann I, Schenkl S, Buckle R, Kaatz M. Clinical two-photon microendoscopy. Microscopy Research and Technique. 2007;70:398–402.
[28] König K. Clinical multiphoton tomography. Journal of Biophotonics. 2008;1:13–23.
[29] Graf BW, Jiang Z, Tu H, Boppart SA. Dual-spectrum laser source based on fiber continuum generation for integrated optical coherence and multiphoton microscopy. Journal of Biomedical Optics. 2009;14.
[30] Breunig HG, Studier H, König K. Multiphoton excitation characteristics of cellular fluorophores of human skin in vivo. Optics Express. 2010;18:7857–7871.
[31] Wang BG, König K, Halbhuber KJ. Two-photon microscopy of deep intravital tissues and its merits in clinical research. Journal of Microscopy. 2010;238:1–20.
[32] Koehler MJ, Vogel T, Elsner P, Konig K, Buckle R, Kaatz M. In vivo measurement of the human epidermal thickness in different localizations by multiphoton laser tomography. Skin Research and Technology. 2010;16:259–264.
[33] König K. High-resolution multimodal clinical multiphoton tomography of skin. Progress in Biomedical Optics and Imaging – Proc SPIE 7883; 2011. p. 78830D-1.
[34] Benati E, Bellini V, Borsari S, Dunsby C, Ferrari C, French P, Guanti M, Guardoli D, Koenig K, Pellacani G, et al. Quantitative evaluation of healthy epidermis by means of multiphoton microscopy and fluorescence lifetime imaging microscopy. Skin Research and Technology. 2011; 17:295–303.
[35] Liang X, Graf BW, Boppart SA. In vivo multiphoton microscopy for investigating biomechanical properties of human skin. Cellular and Molecular Bioengineering. 2011;4:231–8.
[36] Graf BW, Boppart SA. Multimodal in vivo skin imaging with integrated optical coherence and multiphoton microscopy. IEEE Journal on Selected Topics in Quantum Electronics. 2012;18: 1280–1286.
[37] Seidenari S, Arginelli F, Bassoli S, Cautela J, French PMW, Guanti M, Guardoli D, König K, Talbot C, Dunsby C. Multiphoton laser microscopy and fluorescence lifetime imaging for the evaluation of the skin. Dermatology Research and Practice. 2012:810749.
[38] Decencière E, Tancrède-Bohin E, Dokladal P, Koudoro S, Pena AM, Baldeweck T. Automatic 3D segmentation of multiphoton images: A key step for the quantification of human skin. Skin Research and Technology. 2013;19:115–124.
[39] Balu M, Mazhar A, Hayakawa CK, Mittal R, Krasieva TB, König K, Venugopalan V, Tromberg BJ. In vivo multiphoton NADH fluorescence reveals depth-dependent keratinocyte metabolism in human skin. Biophysical Journal. 2013;104:258–267.

[40] Weinigel M, Breunig HG, Fischer P, Kellner-Höfer M, Bückle R, König K. Clinical multiphoton endoscopy with FLIM capability. Progress in Biomedical Optics and Imaging – Proc SPIE 8588; 2013.
[41] Wang H, Lee AMD, Frehlick Z, Lui H, McLean DI, Tang S, Zeng H. Perfectly registered multiphoton and reflectance confocal video rate imaging of in vivo human skin. Journal of Biophotonics. 2013;6:305–309.
[42] Koenig K, Weinigel M, Breunig HG, Uchugonova A. Quantitative multiphoton imaging. Progress in Biomedical Optics and Imaging – Proc SPIE 8948; 2014.
[43] Yew E, Rowlands C, So PTC. Application of multiphoton microscopy in dermatological studies: a mini-review. Journal of Innovative Optical Health Sciences. 2014;7(5):1330010.
[44] Darvin ME, Richter H, Zhu YJ, Meinke MC, Knorr F, Gonchukov SA, König K, Lademann J. Comparison of in vivo and ex vivo laser scanning microscopy and multiphoton tomography application for human and porcine skin imaging. Quantum Electron. 2014;44:646–651.
[45] König K. Hybrid multiphoton multimodal tomography of in vivo human skin. IntraVital. 2012;1: 11–26.
[46] Koehler MJ, Konig K, Elsner P, Buckle R, Kaatz M. In vivo assessment of human skin aging by multiphoton laser scanning tomography. Optics Letters. 2006;31:2879–2881.
[47] Koehler MJ, Hahn S, Preller A, Elsner P, Ziemer M, Bauer A, Konig K, Buckle R, Fluhr JW, Kaatz M. Morphological skin aging criteria by multiphoton laser scanning tomography: Non-invasive in vivo scoring of the dermal fibre network. Experimental Dermatology. 2008;17:519–523.
[48] Koehler MJ, Preller A, Kindler N, Elsner P, König K, Bückle R, Kaatz M. Intrinsic, solar and sunbed-induced skin aging measured in vivo by multiphoton laser tomography and biophysical methods. Skin Research and Technology. 2009;15:357–363.
[49] Kaatz M, Sturm A, Elsner P, König K, Bückle R, Koehler MJ. Depth-resolved measurement of the dermal matrix composition by multiphoton laser tomography. Skin Research and Technology. 2010;16:131–136.
[50] Baldeweck T, Tancrède E, Dokladal P, Koudoro S, Morard V, Meyer F, Decencière E, Pena AM. In vivo multiphoton microscopy associated to 3D image processing for human skin characterization. Progress in Biomedical Optics and Imaging – Proc SPIE 8226; 2012.
[51] Koehler MJ, Preller A, Elsner P, König K, Hipler UC, Kaatz M. Non-invasive evaluation of dermal elastosis by in vivo multiphoton tomography with autofluorescence lifetime measurements. Experimental Dermatology. 2012;21:48–51.
[52] Puschmann S, Rahn CD, Wenck H, Gallinat S, Fischer F. Approach to quantify human dermal skin aging using multiphoton laser scanning microscopy. Journal of Biomedical Optics. 2012; 17:036005.
[53] Sanchez WY, Obispo C, Ryan E, Grice JE, Roberts MS. Erratum: Changes in the redox state and endogenous fluorescence of in vivo human skin due to intrinsic and photo-aging, measured by multiphoton tomography with fluorescence lifetime imaging. Journal of Biomedical Optics. 2013;18(6):069802.
[54] Miyamoto K, Kudoh H. Quantification and visualization of cellular NAD(P)H in young and aged female facial skin with in vivo two-photon tomography. British Journal of Dermatology. 2013; 169:25–31.
[55] Darvin ME, Richter H, Ahlberg S, Haag SF, Meinke MC, Le Quintrec D, Doucet O, Lademann J. Influence of sun exposure on the cutaneous collagen/elastin fibers and carotenoids: Negative effects can be reduced by application of sunscreen. Journal of Biophotonics. 2014;7:735–743.
[56] Leppert J, Krajewski J, Kantelhardt SR, Schlaffer S, Petkus N, Reusche E, Hüttmann G, Giese A. Multiphoton excitation of autofluorescence for microscopy of glioma tissue. Neurosurgery. 2006;58:759–767.

[57] König K, Speicher M, Bückle R, Reckfort J, McKenzie G, Welzel J, Koehler MJ, Elsner P, Kaatz M. Clinical optical coherence tomography combined with multiphoton tomography of patients with skin diseases. Journal of Biophotonics. 2009;2:389–397.
[58] Dimitrow E, Riemann I, Ehlers A, Koehler MJ, Norgauer J, Elsner P, König K, Kaatz M. Spectral fluorescence lifetime detection and selective melanin imaging by multiphoton laser tomography for melanoma diagnosis. Experimental Dermatology. 2009;18:509–515.
[59] Dimitrow E, Ziemer M, Koehler MJ, Norgauer J, König K, Elsner P, Kaatz M. Sensitivity and specificity of multiphoton laser tomography for in vivo and ex vivo diagnosis of malignant melanoma. Journal of Investigative Dermatology. 2009;129:1752–1758.
[60] Paoli J, Smedh M, Ericson MB. Multiphoton laser scanning microscopy – a novel diagnostic method for superficial skin cancers. Seminars in Cutaneous Medicine and Surgery. 2009;28: 190–195.
[61] König K, Speicher M, Kohler MJ, Scharenberg R, Kaatz M. Clinical application of multiphoton tomography in combination with high-frequency ultrasound for evaluation of skin diseases. Journal of Biophotonics. 2010;3:759–773.
[62] Huck V, Gorzelanny C, Thomas K, Niemeyer V, Luger TA, Konig K, Schneider SW. Intravital multiphoton tomography as a novel tool for non-invasive in vivo analysis of human skin affected with atopic dermatitis. Progress in Biomedical Optics and Imaging – Proc SPIE 7548; 2010.
[63] Huck V, Gorzelanny C, Thomas K, Mess C, Dimitrova V, Schwarz M, Riemann I, Niemeyer V, Luger TA, König K, et al. Intravital multiphoton tomography as an appropriate tool for non-invasive in vivo analysis of human skin affected with atopic dermatitis. Progress in Biomedical Optics and Imaging – Proc SPIE 7883; 2011.
[64] Koehler MJ, Speicher M, Lange-Asschenfeldt S, Stockfleth E, Metz S, Elsner P, Kaatz M, Konig K. Clinical application of multiphoton tomography in combination with confocal laser scanning microscopy for in vivo evaluation of skin diseases. Experimental Dermatology. 2011;20: 589–594.
[65] Koehler MJ, Zimmermann S, Springer S, Elsner P, König K, Kaatz M. Keratinocyte morphology of human skin evaluated by in vivo multiphoton laser tomography. Skin Research and Technology. 2011;17:479–486.
[66] Seidenari S, Arginelli F, Dunsby C, French P, König K, Magnoni C, Manfredini M, Talbot C, Ponti G. Multiphoton laser tomography and fluorescence lifetime imaging of basal cell carcinoma: Morphologic features for non-invasive diagnostics. Experimental Dermatology. 2012;21: 831–836.
[67] Seidenari S, Arginelli F, Bassoli S, Cautela J, Cesinaro AM, Guanti M, Guardoli D, Magnoni C, Manfredini M, Ponti G, et al. Diagnosis of BCC by multiphoton laser tomography. Skin Research and Technology. 2013;19:e297–e304.
[68] Patalay R, Talbot C, Alexandrov Y, Lenz MO, Kumar S, Warren S, Munro I, Neil MAA, König K, French PMW, et al. Multiphoton Multispectral Fluorescence Lifetime Tomography for the Evaluation of Basal Cell Carcinomas. PLoS ONE. 2012;7:e43460.
[69] Balu M, Kelly KM, Zachary CB, Harris RM, Krasieva TB, König K, Tromberg BJ. Clinical studies of pigmented lesions in human skin by using a multiphoton tomograph, Progress in Biomedical Optics and Imaging – Proc SPIE 8588; 2013. p. 858812-1–858812-6.
[70] Ulrich M, Klemp M, Darvin ME, König K, Lademann J, Meinke MC. In vivo detection of basal cell carcinoma: Comparison of a reflectance confocal microscope and a multiphoton tomograph. Journal of Biomedical Optics. 2013;18:061229-1–061229-7.
[71] Balu M, Kelly KM, Zachary CB, Harris RM, Krasieva TB, König K, Durkin AJ, Tromberg BJ. Distinguishing between benign and malignant melanocytic nevi by in vivo multiphoton microscopy. Cancer Research. 2014;74:2688–2697.

[72] König K, Ehlers A, Stracke F, Riemann I. In vivo drug screening in human skin using femtosecond laser multiphoton tomography. Skin Pharmacology & Physiology. 2006;19:78–88.
[73] Stracke F, Weiss B, Lehr C-M, König K, Schaefer UF, Schneider M. Multiphoton microscopy for the investigation of dermal penetration of nanoparticle-borne drugs. Journal of Investigative Dermatology. 2006;126:2224–2233.
[74] Schenke-Layland K, Riemann I, Damour O, Stock UA, Konig K. Two-photon microscopes and in vivo multiphoton tomographs – Powerful diagnostic tools for tissue engineering and drug delivery [Review]. Advanced Drug Delivery Reviews. 2006;58:878–896.
[75] Le Harzic R, Colonna A, Bückle R, Ehlers A, Hadjur C, Leroy F, Flament F, Bazin R, Piot B, Riemann I, et al. In vivo multiphoton tomography: a non invasive powerful tool for biochemical investigation of human skin. Proc SPIE 6630; 2007. p. 66300V-7.
[76] Zvyagin AV, Zhao X, Gierden A, Sanchez W, Ross JA, Roberts MS. Imaging of zinc oxide nanoparticle penetration in human skin in vitro and in vivo. Journal of Biomedical Optics. 2008;13:064031.
[77] Bazin R, Flament F, Colonna A, Le Harzic R, Buckle R, Piot B, Laize F, Kaatz M, Konig K, Fluhr JW. Clinical study on the effects of a cosmetic product on dermal extracellular matrix components using a high-resolution multiphoton tomograph. Skin Research and Technology. 2010;16: 305–310.
[78] König K, Raphael AP, Lin L, Grice JE, Soyer HP, Breunig HG, Roberts MS, Prow TW. Applications of multiphoton tomographs and femtosecond laser nanoprocessing microscopes in drug delivery research. Advanced Drug Delivery Reviews. 2011;63:388–404.
[79] Roberts MS, Dancik Y, Prow TW, Thorling CA, Lin LL, Grice JE, Robertson TA, Konig K, Becker W. Non-invasive imaging of skin physiology and percutaneous penetration using fluorescence spectral and lifetime imaging with multiphoton and confocal microscopy. European Journal of Pharmaceutics and Biopharmaceutics. 2011;77:469–488.
[80] Darvin ME, Konig K, Kellner-Hoefer M, Breunig HG, Werncke W, Meinke MC, Patzelt A, Sterry W, Lademann J. Safety assessment by multiphoton fluorescence/second harmonic generation/hyper-Rayleigh scattering tomography of ZnO nanoparticles used in cosmetic products. Skin Pharmacology and Physiology. 2012;25:219–226.
[81] Leite-Silva VR, Lamer ML, Sanchez WY, Liu DC, Sanchez WH, Morrow I, Martin D, Silva HDT, Prow TW, Grice JE, et al. The effect of formulation on the penetration of coated and uncoated zinc oxide nanoparticles into the viable epidermis of human skin in vivo. European Journal of Pharmaceutics and Biopharmaceutics. 2013;84:297–308.
[82] Sugata K, Osanai O, Sano T, Takema Y. Evaluation of photoaging in facial skin by multiphoton laser scanning microscopy. Skin Research and Technology. 2011;17:1–3.
[83] Del Bino S, Sok J, Bessac E, Bernerd F. Relationship between skin re-sponse to ultraviolet exposure and skin color type. Pigment Cell Research. 2006;19:606–614.